AUTOMATIC DETECTION OF HARD EXUDATES AND OPTIC DISC IN DIGITAL FUNDUS IMAGES

Elizabeth Chavez-Hernandez[1] and M. Elena Martinez-Perez[2]

[1]*Postgraduate Program in Computer Science and Engineering, Insituto de Investigaciones en Matemáticas Aplicadas y en Sistemas, Universidad Nacional Autónoma de México, 04510 México City, México*

[2]*Department of Computer Science, Instituto de Investigaciones en Matemáticas Aplicadas y en Sistemas Universidad Nacional Autónoma de México, Apartado Postal 20-726, 04510 México City, México*

Keywords: Hard exudates, Optic disc, Segmentation, Retinal images.

Abstract: Automatic detection of characteristic patterns of diabetic retinopathy such as hard exudates may help to an early diagnosis. Methods for automatic detection of hard exudates and optic disc are presented. Exudates detection involves a preprocessing stage, threshold selection and region growing. For optic disc detection a Bayes classifier is applied followed by mathematical morphology techniques in order to improve the final result. The methods here presented were evaluated using the IMAGERET database, which contains fundus images evaluated by qualified experts. In average, the area of exudates automatically detected overlaped with 60.75% and 63.91% areas defined by each of the two experts. For optic disc detection, sensitivity and specificity were 72.12% and 95.56% respectively.

1 INTRODUCTION

Diabetes Mellitus (DM) has became a public health problem worldwide. Diabetic retino- pathy (DR) is an illness that affects blood vessels in the retina, and it is directly correlated with evolution time of DM and if it is not early detected may cause partial or even total blindness (Pereira Delgado, 2005). One of the observed patterns in fundus images of RD patients are the hard exudates, shinny and yellowish intraretinal protein deposits of irregular shape. The optic disc (OD) is observed with similar intensities as the exudates but its shape is more regular and it does not represent a pathological sign. Detection of OD is an important step in developing systems for automatic diagnosis of various serious ophthalmic pathologies. There are previous works related with the detection of exudates such as those based on a combination of local and global thresholding (Phillips et al., 1993); color normalization, local contrast enhancement followed by a fuzzy C-means clustering and neural networks (Osareh et al., 2001); finally those based on recursive region growing thechnique (Sinthanayothin et al., 1999). For OD detection methods can be grouped into three types: i) related with location, generally representative of its center (Foracchia et al., 2004); ii) templated-based methods to obtein OD boundary approximation (Wong et al., 2008); and iii) based on deformable models or snakes (Xu et al., 2007). In this work, we present an alternative methodology for hard exudates and optic disc detection. Segmentation preliminary results are evaluated using the public database IMAGERET-DIARETDB1 V2.1 (Kauppi et al., 2009).

2 HARD EXUDATES RECOGNITION

In order to reduce the shade effect of the non uniform lightening, a process of contrast correction is needed (Fleming et al., 2006). First, a 3×3 pixels median filter is applied to the green component of the RGB image, followed by a gaussian filter with $\sigma = 2$, the resulting image is called I. Second, a 35×35 pixels median filter is applied to the green component of the original RGB image, calling G' to this image. Image S' is calculated by $S' = I/G' - 1$, and finally, contrast corrected image is obtained after normalizing S' by its standard deviation, $S = S'/std(S')$ (Figure 1b).

2.1 Threshold Selection and Region Growing

The objective of the first stage of our method is to

Chavez-Hernandez E. and Elena Martinez-Perez M..
AUTOMATIC DETECTION OF HARD EXUDATES AND OPTIC DISC IN DIGITAL FUNDUS IMAGES.
DOI: 10.5220/0003890905430547
In *Proceedings of the International Conference on Bio-inspired Systems and Signal Processing* (MIAD-2012), pages 543-547
ISBN: 978-989-8425-89-8

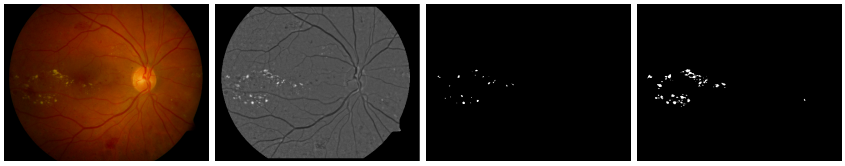

(a) (b) (c) (d)

Figure 1: (a) Original images (S). (b) Contrast correction of image. (c) Binary image resulted by the threshold method ($BW1$). (d) Final recognition of hard exudates.

find an optimal threshold t that discriminates between two classes of pixels, the *background*, and *exudates*. For this purpose the Otsu method (Otsu, 1979) is applied to identify a threshold t_0. In order to minimize false positives this step is repeated a second time over the region with intensities higher than t_0, resulting in a threshold value t. The binary image with threshold t is called $BW1$ (Figure 1c). To improve exudates detection and correct for the underselection, $BW1$ image is considered as seed regions for exudates, $BW1$ is then dilated by 15 pixels, and the followed criterion is applied for every pixel $p(i,j)$ in the dilated region,

$$p_{(i,j)} = \begin{cases} exudate & \text{if} \quad p \geq (t-2s) \\ background & \text{if} \quad p < (t-2s) \end{cases} \tag{1}$$

where t is threshold found in the first stage and s, the standard deviation of seed pixels defined by $BW1$. By this, candidate pixels with intensities greater than $t-2s$ are classified as *exudates* and, pixels with intensities below this, are classified as *background* (Figure 1d).

3 OPTIC DISC DETECTION

3.1 Bayes Classifier

A Bayes classifier is applied in order to obtain a binary image with only two classes of pixels, the so called *disc* and *background*. Probabilities are calculated using training images on which the class for each pixel is known, as defined by experts. The probability of a pattern to belong to the class C_k is obtained as:

$$p(C_k \mid x) = \frac{p(x \mid C_k)p(C_k)}{p(x)} \tag{2}$$

Assigning a pattern x to the class with the highest *a posteriori* probability minimises the error probability, then, we assign a pattern x to a class if:

$$p(C_k \mid x) > p(C_j \mid x) \qquad \forall j \neq k \tag{3}$$

The first step was then to choose a set of images to train the classifier, for this purpose 10 images were randomly chosen from the database IMAGERET (Kauppi et al., 2009). The characteristics considered for the training step were the following:

1. Red band of the original RGB image,called R.
2. Green band of the original RGB image, called G.
3. Variance image of G, this is calculated as in (Sinthanayothin et al., 1999), a subimage $W(i,j)$ is defined centered in the pixel (i,j) of dimensions $M \times M$. Let $\langle f \rangle_{W(i,j)}$ be the mean intensity in $W(i,j)$. The variance image is given by:
$$V(i,j) = \langle f^2 \rangle_W - (\langle f \rangle_W)^2 \tag{4}$$
where f represents pixel intensity on image G.
4. Value of y axis of pixels on the optic disc, since optic disc is showed in the central section of images.

Once the training step has finished, the classifier should get an image as input and return a binary image, called $BW2$ (Figure 2b). However, other techniques are required to accurately define the OD.

3.2 Mathematical Morphology

The second stage on optic disc recognition involves mathematical morphology in order to discriminate the OD among the other regions showed as the result of previous stage. First, a morphological aperture is applied, this operation removes those clusters with few pixels. Next, a closure is applied using a disc as structural element in order to eliminate hypointense regions within the larger clusters in the image. Finally holes are filled in the clusters on the image. This dark branches in the OD are due to the blood vessels that appear as dark areas in the image.

After these operations, the image contains clusters of different sizes, for each of these objects the area and its roundness is calculated. Roundness is obtained through,

$$roundness(k_i) = \frac{4\pi A_{k_i}}{P_{k_i}^2} \tag{5}$$

where A_{k_i} is the area of object i and P_{k_i} is the perimeter of the same object. The optic disc will be that

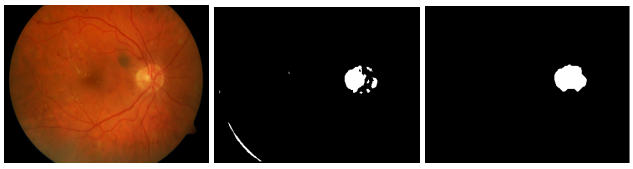

(a) (b) (c)

Figure 2: (a) Original image. (b) Result of Bayes classifier ($BW2$). (c) Final recognition of optic disc.

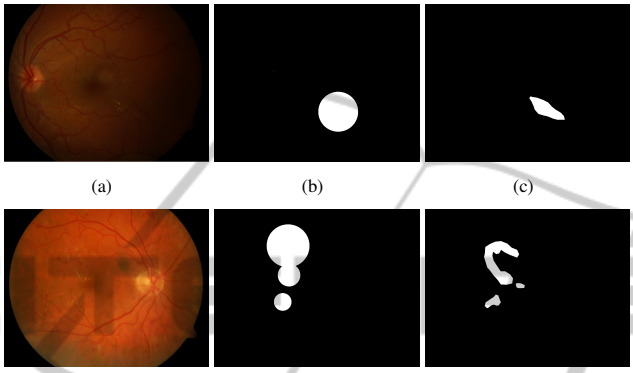

(a) (b) (c)

(d) (e) (f)

Figure 3: (a) and (d) Original images. (b) and (e) Hard exudates found by Expert 1. (c) and (f) Hard exudates found by Expert 2.

object whose roundness is greater than 0.8 and area greater than 1.5% of the image (Figure 2c). All parameter values, constants and windows sizes given along the description of the methodology refer to images of 1150×1500 size in pixels. For different image resolutions, all of these values have to be scaled.

4 EVALUATION

For evaluation of exudates and OD recognition, the image database IMAGERET (Kauppi et al., 2009) was used, this database is open access and available on the web. We used 25 fundus images from this database where images have been evaluated by experts, each of them highlighting gross areas where the experts recognize one of the following patterns: hard exudates, soft exudates, haemorrhages and red small dots. The database comes with a Matlab toolkit that allows to explore annotations by experts. Figure 3 shows examples of two images with hard exudates from the database and its annotations by experts.

Experts were asked to highlight the areas where the pattern of interest is found using a circle, ellipse or a polygon region. From Figure 3, it can be seen that there are differences between the exudates selected by different experts, in fact, in some cases there is no coincidence in the areas detected as containing exudates. As definition, methods of the experts are based in gross detection and their results are not comparable to the methods presented here, which define the structures more precisely. Because of that, evaluation was based on the percentage of the area of exudates detected contained in the areas defined by experts. There are cases in which automatic detection of exudates is evaluated as very good, for example in image 13 showed in Figure 4a, since exudates detected are fully contained within the area defined by the experts. However, in image 27, showed in Figure 4e, one expert doesn't reports exudates while the other reports an area that only overlap with 1.63% of exudates reported by our results.

This incongruences doesn't necessarily means that automatic recognition has been poor, in the case of image 27, it contains some patterns with intensities very similar to those of exudates which are probably due to a treatment that causes scars in the retina. In average, for the 25 images evaluated, the area of exudates detected by the methods here presented that is within the area defined by expert 1 is 60.75%, and 63.91% for expert 2, as shown on Table 1. For OD evaluation, contingency tables were used, and so, sensitivity and specificity were evaluated according to,

$$Sensitivity = \frac{VP}{VP+FN} \qquad Specificity = \frac{VN}{VN+FP} \tag{6}$$

where VP represents the true positives, VN the true negatives, FP the false positives and FN the false

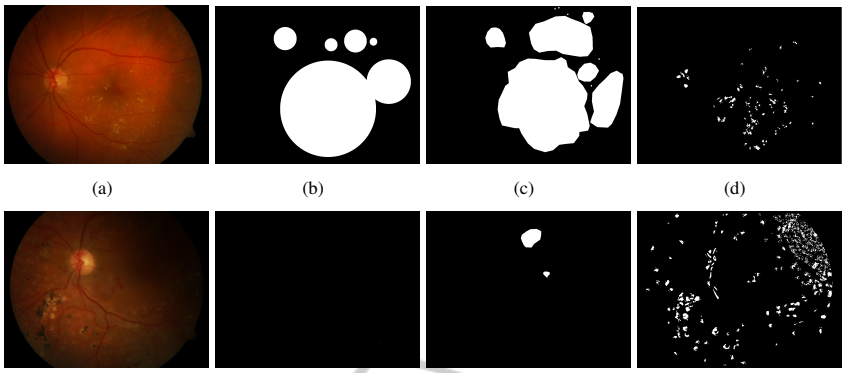

Figure 4: (a) and (e) Original images. (b) and (f) Hard exudates found by Expert 1. (c) and (g) Hard exudates found by Expert 2. (d) and (h) Hard exudates found by our method.

Table 1: Results for evaluation of automatic detection of exudates and optic disc. The average area of exudates overlapped with the areas highlighted by the experts is presented. Sensitivity and specificity is shown for optic disc detection.

	Hard exudates		Optic Disc	
	Expert 1	Expert 2	Sensitivity	Specificity
Mean	60.75%	63.91%	72.12%	95.56%

negatives number of pixels respectively . In Table 1 results for sensitivity and specificity are shown for 25 images from IMAGERET (Kauppi et al., 2009) database. In average, our methods detect the OD with sensitivity of 72.12% and specificity of 95.56%.

Ideally, the evaluation of exudates should be done similar to that of the optic disc, however the database we used does not allow us to make that assessment. It is not possible to compare our preliminary results with other studies since most of these works used their own databases which are not public. It is necessary therefore the generation of a public database of patterns marked by experts accurately for a reliable evaluation and comparison.

5 CONCLUSIONS

Methods for automatic detection of hard exudates and optic disc in fundus images were presented. These methods preserved computational simplicity, still achieving good results even for images with a wide range of lightening conditions. Differences in the selection of exudates by the experts and methods here presented complicated the definition of good evaluation techniques. Selection of the optic disc by the experts was more specific, allowing a better evaluation of concordance. From our preliminary results we concluded that a more pattern specific public database make by experts is needed in order to have a more reliable evaluation. Work is being done in this issue.

REFERENCES

Fleming, A., Philip, S., Goatman, K., Olson, J., and Sharp, P. (2006). Automated microaneurysm detection using local contrast normalization and local vessel detection. *IEEE Transactions on Medical Imaging*, 25(9):1223–1232.

Foracchia, M., Grisan, E., and Ruggeri, A. (2004). Detection of optic disc in retinal images by means of a geometrical model of vessel. *IEEE Trans. Med. Imag.*, 23(10):1189–1195.

Kauppi, T., Kalesnykiene, V., Kamarainen, J., Lensu, L., and et. al. (2009). Imageret-database. *www2.it.lut.fi/project/imageret/*.

Osareh, A., Mirmehdi, M., Thomas, B., and Markham, R. (2001). Automatic recognition of exudative maculopathy using fuzzy c-means clustering and neural networks. *In Proc Medical Image Understanding and Analysis*, pages 49–52.

Otsu, N. (1979). A threshold selection method from gray-level histograms. *IEEE Trans. Syst., Man, Cybern.*, 9:62–66.

Pereira Delgado, E. (2005). *Nuevas perspectivas en oftalmología: Retinopatía diabética*. Glosa, Laboratorios Esteve.

Phillips, R., Forrester, J., and Sharp, P. (1993). Automated detection and quantification of retinal exudates. *Graefe's Archive for Clinical and Experimental Ophthalmology*, 231(2):90–94.

Sinthanayothin, C., Boyce, J., Cook, H., and Williamson, T. (1999). Automated localization of the optic disc, fovea, and retinal blood vessels from digital colour fundus images. *British Journal of Ophthalmology*, 83(8):902–910.

Wong, D. W. K., Liu, J., Lim, J. H., Jia, X., Yin, F., Li, H., and Wong, T. Y. (2008). Level-set based automatic

cup-to-disc ratio determination using retinal fundus images in ARGALI. *In Proc. 30th Annu. Int. IEEE EMBS Conf.*, pages 2266–2269.

Xu, J., Chutatape, O., Sung, E., Zheng, C., and Kuan, P. C. T. (2007). Optic disk feature extraction via modified deformable model technique for glaucoma analysis. *Pattern Recognition*, 40(7):2063–2076.